**Proceedings of the Korean Nuclear Society Spring Meeting**
**Cheju, Korea, May 1996**

# Analysis of Sintering Behaviors in Er-doped $UO_2$

**Han Soo Kim, Si Hyung Kim, Sang Ho Na, Young Woo Lee, Dong Seong Sohn**

Abstract

Defect equilibrium equations were modelled, and the relations of $p_{O_2}$ *versus* $x$ were derived using the mass action law. The dominant defect species active in a specified region were determined by fitting the curve of experimental data to the calculated curve of log $p_{O_2}$ versus log $x$ for each theoretical model. The calculated curve for (2:1:2) and $(Er'U^{\cdot})^x$ in the hyperstoichiometric $U_{1-y}Er_yO_{2+x}$ and that for $(2Er'V_O^{\cdot\cdot})^x_{dec}$ in the hypostoichiometric $U_{1-y}Er_yO_{2-x}$ are in good agreement with the present experimental results.

The sintering behavior of Er-doped $UO_2$ is observed with erbium content in oxidizing and reducing atmospheres. For sintering in oxidizing atmosphere, sintered density decreases as increasing y in $U_{1-y}Er_yO_{2+x}$. However, in hydrogen atmosphere, sintered density decreases as increasing y at lower erbium content but the density increases again above y=0.10. In oxidizing sintering conditions, the formation of $(Er'U^{\cdot})^x$ clusters hinders the diffusion of cations, and hence the sinterability of Er-doped $UO_2$ decreases. In reducing atmosphere of Er-doped $UO_2$ for higher Er concent, the oxygen vacancies make $(Er'U^{\cdot})^x$ cluster decompose by charge compensation and the concentration of mobile cations increases, thereby improving the sinterability.

## 1. Introduction

Sintering behavior is an important characteristics of Er-doped $UO_2$ fuel since it controls the physical properties for burnable absorber applications. It is generally known that the self-diffusion coefficient of uranium in $UO_{2+x}$ decreases by doping with cations of lower valency than the uranium ions, and increases with higher valent cations by means of dominant defect. The defect structures on the Er-doped $UO_2$ lattices are formed by the differences in charge and size between host and dopant cations. The defect structures in the oxide fuel play important roles in its nonstoichiometric behavior and thermal processes such as sintering, creep and release of fission products at high temperature [1-3]. The sintering behaviors, oxygen potentials and the defect models of $UO_2$ doped with various cations have been studied by many researchers [4, 5]. None, however has reported on the U-Er-O ternary system.

In the present paper, oxygen potential data were analyzed as the function of $p_{O_2}$, dopant content and mean uranium valence. A thermodynamic approach is taken to analyze defect

clusters at the cation and anion sublattice of $U_{1-y}Er_yO_{2+x}$ solid solutions. Er-doped $UO_2$ compacts were sintered in oxidizing and reducing atmospheres. It is tried interpreting the densification behaviors reasonably in terms of defect models in both hyper- and hypostoichiometric regions, respectively. .

## 2. Sintering Experiments

Erbium-doped $UO_2$ powders were prepared by mechanical blending of $UO_{2.099}$ with weighed amount of $Er_2O_3$ powder. The mixed powders were pressed at 286 MPa into green pellets of about 15mm in diameter and 9mm in length.

Sintering in hydrogen atmosphere was performed at 1700 and 1850 °C for 4 hours. Sintering experiments in oxidizing atmosphere were carried out at 1250 °C for 5 hours. The oxygen partial pressure in the sintering atmosphere was adjusted by the use of $CO_2/CO$ mixture (mixing ratio=6/1) as sintering gas. The pellets sintered in oxidizing atmosphere were followed by reduction in $CO_2/CO$ mixtures at 1250 °C, 4 hours that reduces the pellets to stoichiometry.

## 3. Results and Discussion.

### 3. 1. Mean uranium valence in $U_{1-y}Er_yO_{2+x}$

The mean valence of uranium were calculated assuming the valences of erbium and oxygen in the specimen to be +3 and -2, respectively. The equilibrium among uranium ions and oxygen ions in $UO_{2+x}$ and oxygen gas in the atmosphere is written as follows :

$O^{2-} + 2U^{5+} = 2U^{4+} + \frac{1}{2}O_2(g)$.

When the composition of solid solution is taken as $U_{1-y}Er_yO_{2+x}$, the concentration of cation sites satisfies following equation; $[U^{4+}] + [U^{5+}] = 1-y$, and the electroneutrality condition requires $4[U^{4+}] + 5[U^{5+}] = V_U(1-y)$ and $[O^{2-}] = 2+x = \frac{3}{2}y + \frac{1}{2}V_U(1-y)$, where square brackets is the concentration of each species per total cation site. $V_U$ is the mean valence of the U ion.

### 3. 2. Defect equilibria in $U_{1-y}Er_yO_{2+x}$

#### 3. 2. 1. Modelling of defect structures

In a simple binary oxide system, nonstoichiometric behavior requires metal species to be multivalent to satisfy the electroneutrality with variable cation to anion ratio. Since Er having stable 3+ valence substitutes for $U^{4+}$ in the cubic lattice of the solid solution, negative effective charges and electron holes are created, thereby effectively compensating the charge valence. It is assumed that electron holes combine with nearest host cations, $U^{4+}$, forming $U^{5+}$ ions, i.e. positive polarons.

$Er_U'$ exists as an isolated defect or interacts with the nearest positive polaron at the cation sublattice of the $U_{1-y}Er_yO_{2+x}$ solid solution. The attractive interaction between $Er'$ and $U^{\cdot}$ are assumed to form a dopant-host cation cluster, $(Er'U^{\cdot})^x$. In the hyper -stoichiomtric

region, the present defect thermodynamic formulation is based on the presence of Willis clusters at the anion sublattice and the local dopant-host clusters at the cation sublattice. Therefore, it is considered for this model that the $(Er'U^{\cdot})^{x}$ cluster exists at the cation sublattice and either (2:1:2) or (2:2:2) cluster is a dominant defect at the anion sublattice for the hyperstoichiometric region.

In the hypostoichiometric region, the reduction of solid solution gives rise to oxygen vacancies and electrons. As the number of vacancies increases, Er' ions becomes stabilized by the formation of dopant-vacancy clusters. It is instructive to consider the behaviors of the $(Er'V_O^{\cdot\cdot})^{\cdot}$ and $(2Er'V_O^{\cdot\cdot})^{x}$ models in two different reduction cases, respectively. In the first case, it is considered that the $(Er'U^{\cdot})^{x}$ cluster decomposes into Er' and $U^{\cdot}$ in the hypostoichiometric $U_{1-y}Er_yO_{2-x}$ region. The electrons are localized on positive polarons $U^{\cdot}$ to give normal host cation $U^{x}$, and the charge compensation for $V_O^{\cdot\cdot}$ is thereby maintained. Er' and $V_O^{\cdot\cdot}$ are assumed to interact electrostatically and result in formation of a dopant-vacancy cluster such as $(Er'V_O^{\cdot\cdot})^{\cdot}_{dec}$ or $(2Er'V_O^{\cdot\cdot})^{x}_{dec}$, where 'dec' means decomposition of $(Er'U^{\cdot})^{x}$ cluster. In the second case of reduction, it is assumed that $(Er'V_O^{\cdot\cdot})^{\cdot}_{red}$ or $(2Er'V_O^{\cdot\cdot})^{x}_{red}$ cluster is formed, where 'red' means the electroneutrality condition is satisfied by Er', $V_O^{\cdot\cdot}$ and n'.

The law of mass action and the electroneutrality condition are applied to the defect equilibria including the reactions of gaseous oxygen with defects and the formation of defect clusters in the solid solution. In both hyper- and hypostoichiometric $U_{1-y}Er_yO_{2\pm x}$ solid solutions, the overall electroneutrality is maintained by the formation of positive polarons, dopant-host cation clusters, dopant-oxygen vacancy clusters, oxygen interstitials, oxygen vacancies and electrons. Site filling conditions are deduced on the basis of the assumptions that the number of cations, normal anion sites and interstitial anion sites in the solid solution are the same as in $UO_2$ fluorite structure. Using the site filling conditions, the mass action equations are solved numerically for a range of compositions.

Table 1 shows that the oxygen partial pressure expressed as a function of x, y, m and $\alpha$ for hyperstoichiometry, where m is the effective charge of Willis cluster and $\alpha$ is the mole fraction of dopant involved in the formation of $(Er'U^{\cdot})^{x}$ clusters. The relations of the oxygen partial pressure with x, y and $\beta$ for the hypostoichiometric region are also shown in Table 2, where $\beta$ is the mole fraction of oxygen vacancies involved in the formation of dopant-vacancy clusters in the state of thermodynamic equilibrium for the hypostoichiometric region.

### 3. 2. 2. Dominant defects in $U_{1-y}Er_yO_{2\pm x}$

Nonstoichiometry equations under defect equilibria are expressed as the variation of $p_{O_2}$ with x, y, m and $\alpha$. The change of $p_{O_2}$ is controlled mainly by oxygen composition of solid solution but is also affected by both y and m.

The relations between log $p_{O_2}$ and O/(U+Er) ratio for $U_{0.8}Er_{0.2}O_{2\pm x}$ solid solutions were plotted with curves of different defect species as shown in Fig. 1. It shows that oxygen vacancies are formed below oxygen partial pressure of $10^{-7}$ atmosphere at 1500 ℃ in $U_{0.8}Er_{0.2}O_{2-x}$. The calculated curve for $(2:1:2)^{4'}$ in hyperstoichiometry and that for $(2Er'V_O^{\cdot\cdot})^{x}_{dec}$

in hypostoichiometry are in good agreement with experimental results.

### 3. 3. Analysis of the sintering behaviors of Er-doped $UO_2$

The correlations among defect concentration, mean uranium valence and percent of theoretical densities of sintered pellets are shown in Figs. 2 and 3. For sintering in oxidizing atmosphere, the sintered density decreases as increasing y in $U_{1-y}Er_yO_{2+x}$ though the mean uranium valence increases at higher erbium content as shown in Fig. 2. Each defect concentration in Fig. 2 is obtained from the interpolation of oxygen potential data of $U_{1-y}Er_yO_{2+x}$ solid solutions between 1200 and 1300 °C. At low levels of erbium, $[U^{\cdot}]$ decreases and then increases slightly with erbium content, but $[(Er'U^{\cdot})^x]$ increases continuously. In the case of sintering in oxidizing atmosphere, a number of $U^{\cdot}$ ions are created by charge compensation of oxygen interstitials and lower valent dopant cations. The higher valent uranium ions must be associated with the $Er'$ ions, creating $(Er'U^{\cdot})^x$ clusters. As oxygen potential and dopant content is increased the amount of positive polaron increases and charge imbalence could become neutralized by the formation of $(Er'U^{\cdot})^x$ clusters that effectively hinder the movement of uranium ions except by cooperative transport. The increase of $V_U$ is mainly due to the increase of the concentration of dopant-host cation cluster, therefore the sintering behavior can not be interpreted by $V_U$. The cation diffusivity in $U_{1-y}Er_yO_{2+x}$ is greatly reduced by the formation of $(Er'U^{\cdot})^x$ in oxidizing atmosphere and sintered density is decreased as increasing erbium content under the same sintering conditions of $p_{O_2}$, temperature and time.

Fig. 3 shows the effect of erbium content on the sintered density of Er-doped $UO_2$ pellets after 4 hours at 1700 °C and 1850 °C in hydrogen atmosphere. The defect concentrations in Fig. 3 are obtained by the extrapolation of oxygen potential data of 1500 °C to 1700 °C. Sintered densities decrease as increasing y at lower erbium content but increase above y=0.10. Lower density in the Gd-doped $UO_2$ has also been reported [5, 6].

As shown in Fig. 3, the concentration of dopant-host cation cluster is saturated at higher y, but the concentration of positive polaron, $[U^{\cdot}]$ continuously increases as increasing y. According to valence control rule, substituting $Er^{3+}$ for $U^{4+}$ leads to the increase of the concentration of oxygen vacancies. Under reducing sintering conditions of $U_{1-y}Er_yO_{2-x}$ system, a minimum of $U^{\cdot}$ is created and charge compensation is effected by the creation of oxygen vacancies. The sintering enhancement of Er-doped $UO_2$ pellets over $UO_2$ pellets is due to these oxygen vacancies. The oxygen vacancies make $(Er'U^{\cdot})^x$ cluster decompose and the concentration of mobile cations increase, thereby sinterability is improved for higher erbium content. The effect of erbium content on sinterability in reducing atmosphere, that indicates an imporvement of density above y=0.1, is also consistent with the decomposition of $(Er'U^{\cdot})^x$ cluster.

From the sintering results of both oxidizing and reducing atmospheres, it is clear that the sintering of Er-doped $UO_2$ fuel is very complex and different from $UO_2$. These sintering behaviors are not consistent with the mean uranium valence model but can be interpreted by defect clusters.

## 4. Conclusions

The oxygen potential data agree well with the calculated curve for the $(2{:}1{:}2)^{m\prime}$ model in the whole experimental range of $p_{O_2}$ for $U_{1-y}Er_yO_{2+x}$ solid solutions at 1500 °C. For hypostoichiometric $U_{0.80}Er_{0.20}O_{2-x}$, the curve fitting of experimental data to each theoretical model shows that $(2Er'V_O^{\cdot\cdot})^x_{def}$ is the dominant defect structure.

In oxidizing atmosphere, the $(Er'U^{\cdot})^x$ clusters hinder the movement of uranium ions, and hence the sinterability is decreased. In reducing atmosphere, the charge compensation is affected by the creation of oxygen vacancies. The oxygen vacancies make $(Er'U^{\cdot})^x$ cluster decompose and the concentration of mobile cations increase, thereby the sinterability is improved for higher Er content.

## Reference


[1] T. Matsui and K. Naito, Journal of Less Common Metals, 121 (1986) 279.
[2] P. T. Sawbridge, G. L. Reynolds and B. Burton, J. Nucl. Mater. 97 (1981) 300.
[3] Hj. Matzke, Radiation Effects, 53 (1980) 219.
[4] T. B. Lindemer and J. Brynestad, J. Am. Ceram. Soc. 69 (1986) 867.
[5] K. Une and. M. Oguma, J. Nucl. Mater. 131 (1985) 88.
[6] H. Davis and R. A. Potter, Mater. Sci. Res. 11 (1977) 515.


Table 1. The relations between $p_{O_2}$ and x, site filling conditions and electroneutrality conditions for the dominant defect clusters for hyperstoichiometric $U_{1-y}Er_yO_{2+x}$.

| Dominant defects | Electroneutrality conditions | Site filling conditions | $p_{O_2}$ as a function of x, y, α and m |
|---|---|---|---|
| $O_i''$ - $(Er'U^{\cdot})^x$ model | $[U_U^{\cdot}] = 2[O_i''] + [Er_U']$ | $[O_i^{\cdot}] = x$<br>$[Er_U'] = (1-\alpha)\,y$<br>$[(Er'U^{\cdot})] = \alpha\,y$<br>$[O_O^x] = 2$<br>$[U_U^x] = 1-2y-2x$<br>$[U_U^{\cdot}] = 2x+(1-\alpha)y$ | $\left\{\frac{x\,\alpha^2}{K_{O_2}\,K_{DH}^2\,(1-\alpha)^2\,(1-2x-2y)}\right\}^2$ |
| $(2{:}1{:}2)^{m\prime}$ - $(Er'U^{\cdot})^x$ model | $m[(2{:}1{:}2)^{m\prime}] + [Er_U'] = [U_U^{\cdot}]$ | $[(2{:}1{:}2)^{m\prime}] = x$<br>$[Er_U'] = (1-\alpha)\,y$<br>$[(Er'U^{\cdot})^x] = \alpha y$<br>$[O_O^x] = 2$<br>$[U_U^x] = 1-2y-2x$ | $\left\{\frac{x\,\alpha^m}{4\,K_{212}\,K_{DH}^m\,(1-\alpha)^m\,(1-2y-2x)^m}\right\}^2$ |
| $(2{:}2{:}2)^{m\prime}$ - $(Er'U^{\cdot})^x$ model | $m[(2{:}2{:}2)^{m\prime}] + [Er_U'] = [U_U^{\cdot}]$ | $[O_O^x] = 2$<br>$2[(2{:}2{:}2)^{m\prime}] = x$<br>$[(Er'U^{\cdot})^x] = \alpha y$<br>$[Er_U'] = (1-\alpha)y$<br>$[U_U^{\cdot}] = \frac{mx}{2} + (1-\alpha)y$<br>$[U_U^x] = 1-2y-2x$ | $\frac{x\,\alpha^m}{8\,K_{222}\,K_{DH}^m\,(1-\alpha)^m\,(1-2y-2x)^m}$ |

Table 2. The relations between $p_{O_2}$ and x, site filling conditions and electroneutrality conditions for the dominant defect clusters for hypostoichiometric $U_{1-y}Er_yO_{2-x}$ (x>0).

| Defect model | Electroneutrality conditions | Site filling conditions | $p_{O_2}$ as a function of x, y and β |
|---|---|---|---|
| Decomposition of $(Er'U)^x$ & $(Er'V_O^{\cdot})^{\cdot}$ cluster | $[Er_{U'}] = 2[V_O^{\cdot\cdot}]+[(Er'V_O^{\cdot})^{\cdot}]$ | $[O_O^x] = 2-x$<br>$[V_O^{\cdot\cdot}] = (1-\beta)x$<br>$[(Er'V_O^{\cdot})^{\cdot}] = \beta x$<br>$[(Er'U')^x] = y-2x$<br>$[Er_{U'}] = (2-\beta)x$<br>$[U_U^x] = 1-2y+2x$ | $\left\{\frac{K_{ass}K_{Dvn}(y-2x)^2(2-x)}{(1-2y+2x)^2\beta(2-\beta)x^2}\right\}^2$ |
| Decomposition of $(Er'U)^x$ & $(2Er'V_O^{\cdot})^x$ cluster | $[Er_{U'}] = 2[V_O^{\cdot\cdot}]$ | $[O_O^x] = 2-x$<br>$[V_O^{\cdot\cdot}] = (1-\beta)x$<br>$[(2Er'V_O^{\cdot})^x] = \beta x$<br>$[(Er'U')] = y-(2-\beta)x$<br>$[U_U^x] = 1-2y+(2-\beta)x$ | $\left\{\frac{K_{ass}K_{Dvn}\{y-(2-\beta)x\}^2(2-x)}{\{1-2y+(2-\beta)x\}^2\beta x}\right\}^2$ |
| Reduction of $O_O^x$ & $(Er'V_O^{\cdot})^{\cdot}$ cluster | $n+[Er_{U'}] = 2[V_O^{\cdot\cdot}]+[(Er'V_O^{\cdot})^{\cdot}]$ | $[O_O^x] = 2-x$<br>$[V_O^{\cdot\cdot}] = (1-\beta)x$<br>$[Er'V_O^{\cdot}] = \beta x$<br>$[Er_{U'}] = y-\beta x$<br>$n = y-\beta x$ | $\left\{\frac{K_{RS}K_{Dvn}(2-x)(y-\beta x)}{(2x-y)^2\beta x}\right\}^2$ |
| Reduction of $O_O^x$ & $(2Er'V_O^{\cdot})^x$ cluster | $n+[Er_{U'}] = 2[V_O^{\cdot\cdot}]$ | $[O_O^x] = 2-x$<br>$[V_O^{\cdot\cdot}] = (1-\beta x)$<br>$[(2Er'V_O^{\cdot})^x] = \beta x$<br>$[Er_{U'}] = y-2\beta x$<br>$n = 2x-y$ | $\left\{\frac{K_{RS}K_{Dvn}(2-x)(y-2\beta x)^2}{(2x-y)^2\beta x}\right\}^2$ |

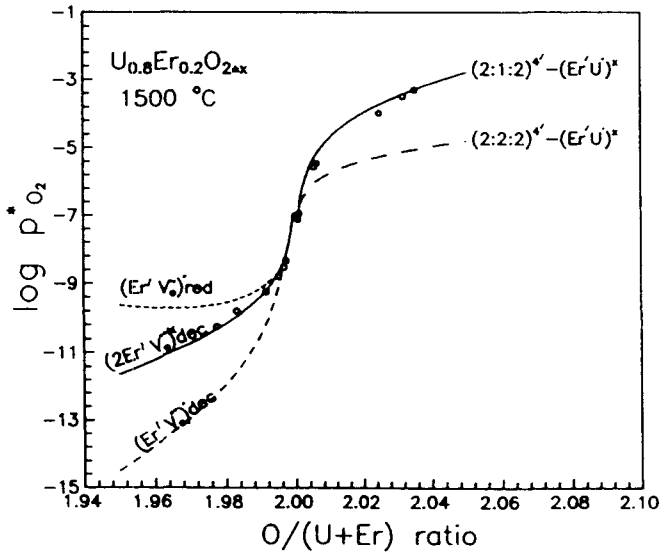


Fig. 1. Comparison of experimental data with various calculated curves for the oxygen partial pressure as a function of $\frac{O}{U+Er}$ ratio for $U_{0.80}Er_{0.20}O_{2\pm x}$ at 1500°C.

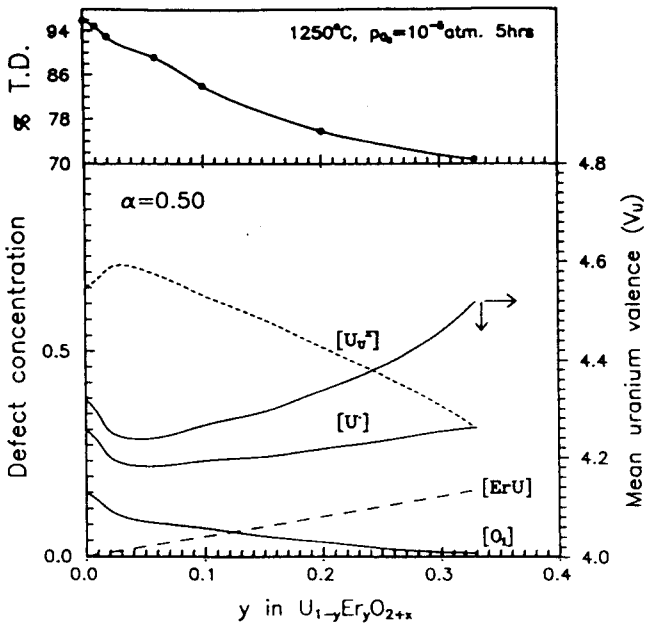


Fig. 2. Correlations among sintered density, defect concentrations and mean uranium valence after sintering in oxidizing atmosphere at 1250°C for 5 hours

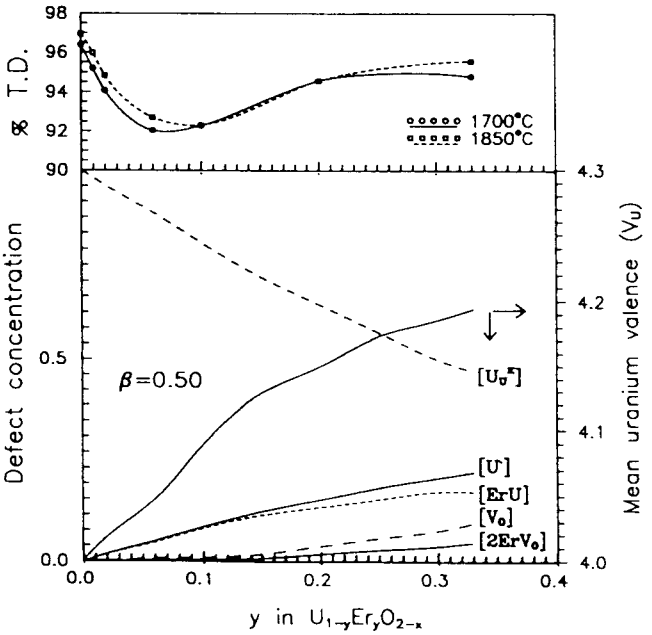


Fig. 3. Correlations among sintered density, defect concentrations and mean uranium valence after sintering in hydrogen at 1700 and 1850°C for 4 hours.